EUROPEAN ORGANIZATION FOR NUCLEAR RESEARCH

CERN-EP/87-71
9 April 1987

# MEASUREMENT OF LASER LIGHT THOMSON-SCATTERED FROM A COOLING ELECTRON BEAM

C. Habfast, H. Poth, B. Seligmann and A. Wolf

Kernforschungszentrum Karlsruhe, Institut für Kernphysik,
Karlsruhe, Fed. Rep. Germany

J. Berger, P. Blatt, P. Hauck, W. Meyer and R. Neumann

Physikalisches Institut, Universität Heidelberg,
Heidelberg, Fed. Rep. Germany

## ABSTRACT

First results are presented from an experiment scattering laser light from a relativistic electron beam. The 5 cm diameter continuous electron beam of 28 keV kinetic energy and 2.6 A current presents an electron gas of a density of $8 \times 10^7$ $cm^{-3}$, from which 20 ns pulses of laser light (490 nm) were scattered at a repetition rate of 15 Hz and an average power of 20 mJ per pulse. The Doppler-shifted wavelength of photons backscattered under 180° was analysed with a Fabry-Perot interferometer. This technique provides, for the first time, a non-destructive measurement of the velocity distribution in an electron beam radially resolved in space. The results presented here comprise the direct measurement of the absolute electron energy and the degree of space-charge compensation in the electron beam. The determination of an upper bound of $10^{-2}$ for the ratio of longitudinal to transverse electron temperature implies the first direct measurement of a flattened velocity distribution.

(Submitted to Applied Physics B)

## 1. INTRODUCTION

The scattering of laser light from a plasma is a frequently applied means of diagnostics. It mainly concerns plasmas of high density (about $10^{13}$ $cm^{-3}$). There it is used to measure continuously the electron temperature. A review on laser diagnostics in plasma research can be found elsewhere [1]. Owing to the low density in electron beams, Thomson scattering as a diagnostics tool was used for beams only in a few cases [2-4]. The densities of the investigated electron beams were in the range from $5 \times 10^{9}$ $cm^{-3}$ to $2 \times 10^{11}$ $cm^{-3}$.

Thomson scattering of laser light from particles is a non-destructive method of diagnostics. Applied to electron beams, it allows the measurement of local electron temperatures and densities by analysing the scattered light in wavelength and intensity. It also provides the possibility of determining the absolute value of the electron energy at any radial position in the electron beam.

We describe here an experiment where laser light was scattered from an electron beam nearly two orders of magnitude less dense than in previous arrangements. The electron beam was generated in an electron cooling device [5] which will be used to cool protons, antiprotons, and possibly other ions stored in the Low Energy Antiproton Ring (LEAR) at CERN. The Thomson scattering diagnostic, proposed for electron cooling devices earlier [6], was applied to investigating the longitudinal energy profile in the electron beam with a radial resolution of about 3 mm and eventually to analysing its longitudinal temperature.

Electron cooling [7] is becoming the essential cooling technique for a number of ion storage rings presently under construction [8]. The development of non-destructive diagnostic methods for cooling electron beams is therefore of general interest. In order to achieve high cooling rates the velocity spread (temperature) within the electron beam must be minimized. Also direct information is required concerning the density distribution and the velocity profile of the electron beam, for which the spatial resolution is needed. There exist various diagnostic methods [9] based on the interaction between the electrons and the stored particles. However, as electron coolers are usually set up and tested separately from the storage ring, one needs methods to optimize the properties of the electron beam prior to their installation.

In the following section details of the experimental set-up are given, in section 3 the data acquisition is described, and in section 4 the relevant electron beam properties are recalled. In section 5 the event rate is

estimated and finally the first results are presented in section 6 followed by the conclusions in section 7.

## 2. EXPERIMENTAL SET-UP

The experimental set-up is schematically shown in Fig. 1. It consists of the LEAR Electron Cooler [5], a dye laser pumped by an excimer laser, and an optical system which separates the backscattered ultraviolet (UV) from the primary visible light and analyses its wavelength. The data of the electron beam and of the laser system are summarized in Tables 1 and 2.

The linearly polarized laser light exits the dye laser and is then displaced so that it is parallel to the electron beam axis, with a horizontal offset of about 40 cm. Before the vacuum window it is brought on axis with the electron beam by means of prisms. One of them is mounted on a horizontally movable sledge. The light enters and leaves the vacuum system of the electron cooler through glass windows mounted under the Brewster angle. Then it is attenuated and hits a photodiode (PD2). Another photodiode (PD1) monitors the laser-pulse intensity by measuring a reflex from an optical element of the beam transport at the exit of the dye laser.

The photons backscattered from the electrons are shifted in wavelength because of the Doppler effect by

$$\lambda_b = \lambda_L(1 + \beta \cos \theta')/(1 + \beta \cos \theta) , \qquad (1)$$

where $\lambda_b$ and $\lambda_L$ are the wavelengths of the backscattered and of the laser light respectively, $\beta$ is the velocity of the electrons in units of the velocity of light, and $\theta$ and $\theta'$ are the angles between incoming and outgoing light and electron beam. For head-on collision ($\theta = 0°$) and exact backscatter ($\theta' = 180°$) this formula reduces to

$$\lambda_b = \lambda_L(1 - \beta)/(1 + \beta) . \qquad (2)$$

The backscattered (UV) light is deflected by a mirror in the vacuum system. The primary laser light passes through a 5 mm hole in the centre of this mirror. The UV light leaves the vacuum system through a quartz window, is again deflected by a mirror, and is focused through a diaphragm. The following optics provides a parallel beam which passes through a plane-parallel Fabry-Perot interferometer (FPI) with a free spectral range of (0.7±0.1) nm at 250 nm. The photons are measured at the end in a solar blind photomultiplier (PM) shielded against visible light by additional wide-band

filters. Light from a low-pressure mercury lamp inflected in front of the diaphragm serves for the adjustment and calibration of the FPI.

## 3. DATA ACQUISITION

The data-acquisition system consisted of an LSI 11/23 computer and NIM and CAMAC electronics. The block diagram is shown in Fig. 2.

The photomultiplier was operated in photon-counting mode. Backscattered photons were detected in coincidence with the laser pulse. This was done in the following way. The excimer laser was triggered by a computer-generated logical pulse. From PD1 a fast signal was derived to define the start of the laser pulse and open the gate (250 ns) for the coincidence with the PM pulse (gated photons). These as well as the ungated PM pulses were counted by CAMAC scalers, which were read out by the computer after a given number of laser pulses. The pulse heights of the photodiodes monitoring the laser pulse intensity were measured with CAMAC analog-to-digital converters (ADCs). The gate for the CAMAC scalers and the ADCs was directly derived from the computer trigger. As the coincidence rate was very low we could inspect the pulse height and timing of each event with a storage oscilloscope. The data read out by the computer (pulse heights of PD1 and PD2, gated and ungated photon rate) were stored on disc and displayed on-line after each cycle of typically $10^4$ laser shots.

## 4. ELECTRON-BEAM PROPERTIES

The investigated electron beam which will be used for cooling has certain properties important for the cooling process. A general description of electron cooling can be found elsewhere [10]. Here we summarize only those aspects relevant to this measurement.

The electron beam is produced with a thermocathode heated to 1050 °C, and is electrostatically accelerated in an electron gun to the desired energy E. The longitudinal electron temperature $T_{\parallel}$ in the beam rest frame of the electrons is related to the FWHM energy spread $\Delta E$ in the laboratory frame by

$$kT_{\parallel} = (1/4)(\Delta E)^2/[E(\gamma+1)] \ , \qquad (3a)$$

where $\gamma = 1/\sqrt{1-\beta^2}$. In a thin electron beam, the energy spread $\Delta E$ is determined by the high-voltage fluctuations dU/U (FWHM) and the cathode temperature $T_C$:

$$\Delta E = \sqrt{(kT_C)^2 + E^2(dU/U)^2} \ . \qquad (3b)$$

The minimum transverse electron temperature in the beam rest frame equals $T_c \approx 0.1$ eV/k. For acceleration energies $E >> kT_c$ as in the present case, the longitudinal temperature assumes much smaller values than the transverse temperature such that the velocity distribution in the beam rest frame is flattened. In a dense electron beam, the actual values of the longitudinal temperature and of $\Delta E$ may be increased by collisions between the electrons which tend to reinstall thermal equilibrium between the longitudinal and transverse degrees of freedom.

The electron beam is transported in a longitudinal magnetic field to prevent radial blow-up due to space charge. Under these conditions one can assume a uniformly distributed electron density $n_e$ across the beam with sharp edges. The space charge leads to a depression of the electric potential on the axis and to a parabolic velocity profile across the beam. The electron energy on the beam axis is

$$E_0 = eU - n_e \pi a^2 r_e mc^2 (1 + 2 \ln b/a) , \qquad (4)$$

where U is the potential difference between the cathode and the vacuum tube surrounding the beam, e the elementary charge, b the radius of the vacuum tube, a the radius of the electron beam, $r_e$ the classical electron radius and m the mass of the electron. The energy varies across the electron beam as

$$E(r) = E_0 + n_e \pi r^2 r_e mc^2 . \qquad (5)$$

The negative charges might be compensated by trapping positive ions in the electron beam. In this case one has to replace $n_e$ by $(1-x)n_e$, where x is a value between zero and one which describes the degree of space-charge compensation. An exact cancellation of the charges would remove the parabolic velocity dependence. In the experiment described here we want to get information about space-charge compensation and longitudinal electron temperature.

## 5. ESTIMATE FOR THE SIGNAL RATE

The expected event rate was previously estimated for the electron cooler under investigation here [11]. It is determined by the well-known differential cross-section for Thomson scattering

$$d\sigma/d\Omega = (1/2) r_e^2 (1 + \cos^2 \Theta') . \qquad (6)$$

For backscattering angles around 180°, $\cos^2 \Theta' \approx 1$. Taking into account the geometrical detection solid angle $\Delta\Omega$, the transformation from the centre-of-mass to the laboratory system, the transmission $\eta$ of the backscattered pho-

tons through the analysing system, and the detection efficiency $\varepsilon$ of the PM, the event rate is given by

$$R = r_e^2 [(1 + \beta)/(1 - \beta)] N_L (n_e/\gamma) \eta \varepsilon \int \Delta\Omega \, dl \, , \qquad (7)$$

where l is the length of the observation volume in the electron beam, and $N_L$ is the number of photons incident from the laser. Since the region from where the photons are backscattered is extended longitudinally, the solid angle of observation depends on the longitudinal coordinate and one has to integrate $\Delta\Omega$ along the longitudinal axis.

The solid angle of the detection system was limited by the diameter of the quartz window (Fig. 1). For the used set-up the integral in Eq. (7) was estimated to be $\Delta\Omega \cdot l = 0.12$ cm, where $\Delta\Omega$ is calculated for the centre of the electron beam. The transmission through the system at 253 nm amounted to 30%, as deduced from the transmission of the optical elements. The measured PM detection efficiency was 12%. This yields an event rate of 0.12 for 1 J of incident laser energy.

## 6. MEASUREMENTS AND RESULTS

The measurements were performed in several steps. First, the photons arriving in the analysing system were counted without having the FPI installed in order to determine the continuous UV photon rate. Wavelength selection was provided by the two wide-band filters. With the laser beam turned off a photon rate of about 500 $s^{-1}$ correlated with the electron beam was observed. These photons may originate from de-excitation of atoms and molecules of the residual gas excited by the electrons. Since the signal rate was measured in coincidence with the laser pulse (gated photon rate) this background was negligible.

The laser beam was then aligned with the electron beam axis. In order to separate Thomson-scattered photons from background ones produced by the laser, data were taken alternately for 500 laser shots ($\approx$ 30 s) with the electron beam at its nominal energy (about 28.3 keV) and the next 500 shots with the electron beam energy 15 keV lower. For technical reasons it was more convenient to step the electron beam down instead of turning it off completely. At lower electron energy the Doppler shift is so small that Thomson-scattered photons were strongly attenuated in the detection system. Moreover, at that energy, the electron beam had a density of only $3 \times 10^7$ $cm^{-3}$. Hence under these conditions only background photons were detected. This procedure permitted one to subtract the background on-line and to become independent of drifts slower than 1 min. Using this procedure,

a total photon rate of typically 20 per 100 J of laser energy containing a background of about 7 was measured. The difference (about 13 photons per 100 J) was attributed to Thomson scattering. The time spectrum of the photons detected in such runs is shown in Fig. 3a. It has a long right-hand tail (late arrivals), which is entirely due to background.

In order to understand the origin of the laser-produced background, a number of checks were performed. We found that the rate was not correlated with the electron beam since it did not change when the electron beam was turned off. Furthermore, no dependence on the residual gas pressure was noted. Finally, it turned out that the background is mainly due to UV photons produced in optical elements, in particular in the rear Brewster window by fluorescence caused by two-photon excitation. This might also explain the late arrivals of the photons (right-hand tail). The time spectrum of the background photons is shown in Fig. 3b.

In order to analyse the wavelength of the photons the FPI was installed. The high tension applied to the acceleration column of the electron gun was controlled within 1 V ($dU/U \approx 3.5 \times 10^{-5}$) and set to such values that, under the assumption of no space-charge compensation in the electron beam, backscattered primary photons of a wavelength very close to 490 nm were Doppler-shifted to a wavelength equal to that of the mercury line (253.652 nm) used to adjust the interferometer. The absolute value of the acceleration voltage was known to $\pm 8$ V and the laser wavelength to $\pm 0.01$ nm. The measurements were performed by scanning the laser wavelength. The result of such scans is shown in Fig. 4. Each point represents an incident laser energy of about 400 J accumulated in $\approx$ 1/2 h. The signals obtained for three slightly different acceleration voltages were fitted by Lorentz curves with common widths and amplitudes. The width of the fitted curves, ($0.05 \pm 0.02$) nm FWHM, is compatible with the experimental resolution dominated by the finesse ($\approx 20$) of the FPI. A change of the high tension produced a shift in the peak position. The observed shift of

$$d\lambda_L/dE = (4.2 \pm 0.6) \times 10^{-3} \text{ nm/eV} \qquad (8)$$

is in reasonable agreement with the expected value of $5.6 \times 10^{-3}$ nm/eV which we use in the following. The signal amplitude, ($0.04 \pm 0.01$) $J^{-1}$, has the expected order of magnitude. Hence, these scans confirm the correct identification of the Thomson-backscattered photons.

The observed peak positions $\lambda_L$ differ from the positions $\lambda_{L,0}$ which can be calculated from Eqs. (2) and (4) assuming vanishing space-charge

compensation and $\lambda_b$ = 253.652 nm. Taking into account the adjacent transmission maxima of the FPI displaced by multiples n of the free spectral range $\Delta\lambda_b$, the degree of space-charge compensation x can be determined from $\lambda_L - \lambda_{L,0}$:

$$x = (\lambda_L - \lambda_{L,0} + n\lambda_L\Delta\lambda_b/\lambda_b)\,(d\lambda_L/dE)^{-1}\,(eU - E_0)^{-1} \quad . \tag{9}$$

Here, $eU - E_0$ is the uncompensated space-charge depression as given in Table 1. The observed differences $\lambda_L - \lambda_{L,0}$ = (1.86 ± 0.03) nm yield three possible values for x, namely

$$\begin{aligned} x &= 0.13 \pm 0.05 \quad (n = -1) \quad , \\ x &= 0.455 \pm 0.01 \quad (n = 0) \quad , \\ x &= 0.8 \pm 0.1 \quad (n = 1) \quad . \end{aligned} \tag{10}$$

The wavelength scans were repeated with an arrangement where the laser beam had been moved parallel, a step of 10 mm away from the electron beam axis. The intention was to observe a shift of the peak due to the parabolic velocity profile of the electron beam. A shifted and broadened signal was found (Fig. 5). The width corresponding to approximately 30 eV can be explained by the spatial resolution being limited to about ±2 mm, mainly by the laser beam diameter. In the centre of the beam, this resolution corresponds to an energy variation of 1.5 eV only, and therefore does not influence the signal width. Signal shifts, calculated from Eqs. (4) and (5) for the three values of x determined previously, are indicated in Fig. 5. By comparison with the observed position of the broadened signal, the lowest value of x obtained for n = -1 is clearly favoured. Hence the measurements indicate that the space-charge compensation in our electron beam is (13 ± 5)%, so that the electron energy is (92 ± 35) eV higher than expected without compensation. Having singled out the order of the FPI transition maximum, we can determine the electron energy under the influence of space charge, from the positions of the observed peaks with a precision of about $10^{-3}$.

The observed line widths confirm that the energy spread of the electrons is smaller than $\Delta E$ = (9 ± 4) eV (FWHM). This implies [see Eq. (3)] that the longitudinal electron beam temperature in the rest frame is lower than $10^{-3}$ eV and therefore at least 100 times smaller than the transverse temperature. This result represents the first direct measurement of a flattened velocity distribution previously deduced only indirectly [12, 13].

## 7. CONCLUSIONS

We have reported on the first observation of laser photons Thomson-scattered from an electron beam generated in an electron cooling device. The observed photon rate is in agreement with our calculations. The background rate was about a factor of 2 lower. It was shown that the wavelength analysis of the backscattered photons permits one to determine the absolute value of the longitudinal electron energy and to put bounds on the longitudinal electron temperature. It further revealed fractional space-charge compensation in the electron beam.

In summary, it was demonstrated that Thomson scattering of pulsed laser light is a useful means of diagnostics for cooling electron beams. For future applications of this method, it is desirable to increase the available laser intensity. This can be realized, for instance, by storing each laser pulse for a number of passages in a confocal resonator [14], placing the electron beam between its cavity mirrors.

### Acknowledgements

This work was supported by the German Bundesministerium für Forschung und Technologie. We would also like to acknowledge the hospitality of the PS-Linac group at CERN and the technical assistance from M. Girardini and J.-L. Vallet.

Thanks are due to the Institute of Physics of the University of Mainz, FRG, for lending us the Fabry-Perot interferometer mechanics.

## REFERENCES


[1] D.E. Evans, Physica 82C, 27 (1976).

[2] V.A. Zhuralev, O.V. Karpov, V.V. Mikheev, V.E. Muzalevskii and G.D. Petrov, Opt. Spektrosk. 57, 997 (1984).

[3] L.E. Dolotov et al., Sov. J. Quantum Electron. 12, 624 (1982).

[4] G. Fiocco and E. Thompson, Phys. Rev. Lett. 10, 89 (1963).

[5] C. Habfast, H. Poth, B. Seligmann, H. Haseroth, C.E. Hill, J.-L. Vallet, and A. Wolf, Status and perspectives of the electron cooling device under construction at CERN, Proc. Third LEAR Workshop on Physics with Cooled Low-Energy Antiprotons in the ACOL Era, Tignes, 1985 (eds. U. Gastaldi, R. Klapisch, J.-M. Richard and J. Tran Thanh Van) (Editions Frontières, Gif-sur-Yvette, 1986), p. 129.

[6] W. Kells, Laser diagnostic, Fermilab Technical Memorandum TM-771 (1978), unpublished.

[7] G.I. Budker and A.N. Skrinsky, Sov. Phys.-Usp. 21, 277 (1978).

[8] Proc. Workshop on Electron Cooling and Related Applications (ECOOL 84) ed. H. Poth, Karlsruhe report KfK 3846 (1985).

[9] P. Moller-Petersen, Diagnostics for electron and ion beam in electron cooling, Ref. [8], p. 219.

[10] H. Poth, Electron cooling, preprint CERN-EP/86-65 (1986), to be published in Proc. CERN Accelerator School, Oxford, 1985.

[11] A. Wolf, Planung eines optischen Systems für die Untersuchung eines Elektronenstrahls durch Thomson-Streuung von Laserlicht, Karlsruhe report, KfK-Primärbericht 11.01.02P17B (1982), unpublished.

[12] G.I. Budker, N.S. Dikansky, V.I. Kudelainen, I.N. Meshkov, V.V. Parchomchuk, D.V. Pestrikov, A.N. Skrinsky and B.N. Sukhina, Part. Accel. 7, 197 (1976);
VAPP-NAP Group (Novosibirsk), Studies on electron cooling of heavy particle beams, report CERN 77-08 (1977);
V.V. Parchomchuk, private communication.

[13] M. Bell, J. Chaney, H. Herr, F. Krienen, P. Moller-Petersen and G. Petrucci, Nucl. Instrum. Methods 190, 237 (1981).

[14] J. Berger, P. Blatt, P. Hauck and R. Neumann, Opt. Commun. 59, 255 (1986).

Table 1

Electron cooler data for this experiment

| | |
|---|---|
| Acceleration voltage U | 28.3 keV |
| Corresponding velocity $\beta$ | 0.32 |
| High-voltage calibration | $\pm$8 V |
| Beam current | (2.57 $\pm$ 0.02 ) A |
| Beam radius a | 2.54 cm |
| Radius of vacuum tube b | 7.0 cm |
| Electron density $n_e$ | 8.2 x $10^7$ $cm^{-3}$ |
| Uncompensated space-charge depression eU - $E_0$ | 730 V |
| Length of interaction region | 1.5 m |
| Typical vacuum in interaction region | 7 x $10^{-10}$ Torr |

Table 2

Typical laser data

| | |
|---|---|
| Excimer laser average power (308 nm) | 6 W |
| Excimer gas | XeCl |
| Repetition rate | 15 Hz |
| Dye laser efficiency | 10% |
| Dye | coumarin 102 |
| Dye tuning range | 470-500 nm |
| Dye laser wavelength calibration | $\pm$0.01 nm |
| Dye laser pulse width | 20 ns |
| Dye laser pulse energy | 40 mJ |
| Dye laser beam diameter | 3 mm |
| Distance from dye laser exit to centre of electron beam | 6 m |
| Transmission from laser exit to electron beam | 50% |
| Number of useful photons per pulse $N_L$ | $5 \times 10^{16}$ |

Figure captions

Fig. 1: Experimental set-up for scattering laser light from a cold electron beam.

Fig. 2: Block diagram of the data-acquisition system.

Fig. 3: Time spectrum of observed photons (arrival time of photons with respect to the leading edge of the laser pulse).

Fig. 4: Thomson-scattered photon rate as a function of laser wavelength in the centre of the electron beam for three values of the acceleration voltage U. Least-squares fit of Lorentz curves with common width, amplitude, and offset.

Fig. 5: Thomson-scattered photon rate as a function of laser wavelength in the centre of the electron beam and at 10 mm distance from the beam axis (acceleration voltage 28280 V).

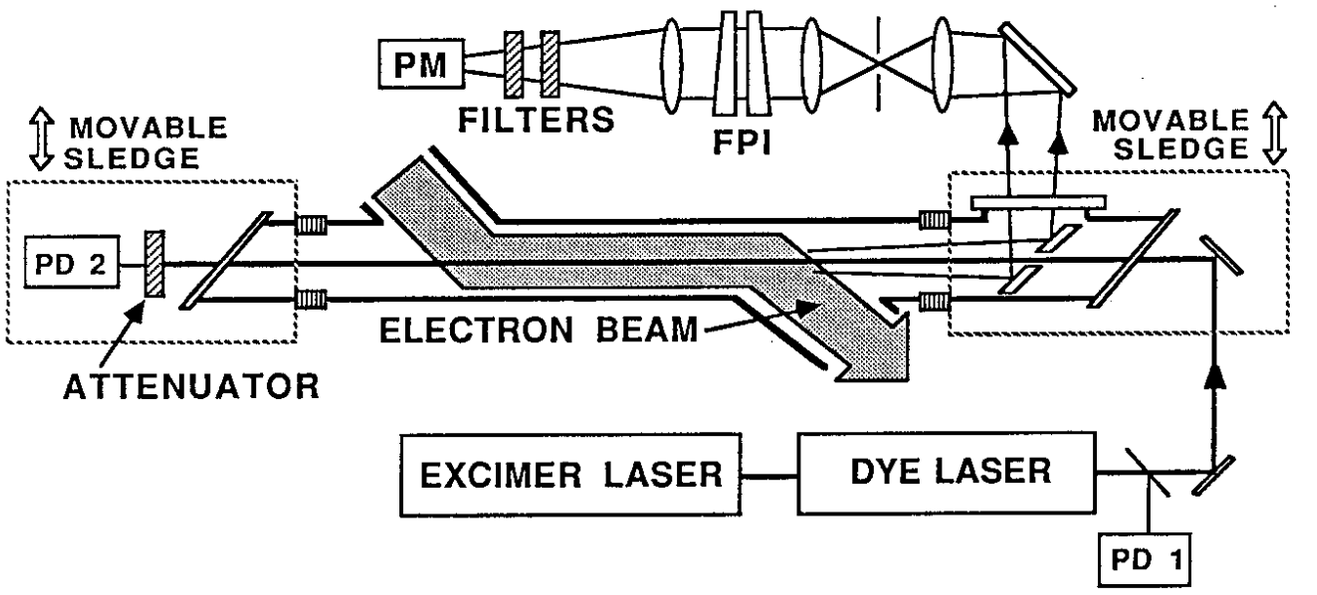
PM
FILTERS
FPI
MOVABLE SLEDGE
MOVABLE SLEDGE
PD 2
ELECTRON BEAM
ATTENUATOR
EXCIMER LASER
DYE LASER
PD 1

Fig. 1

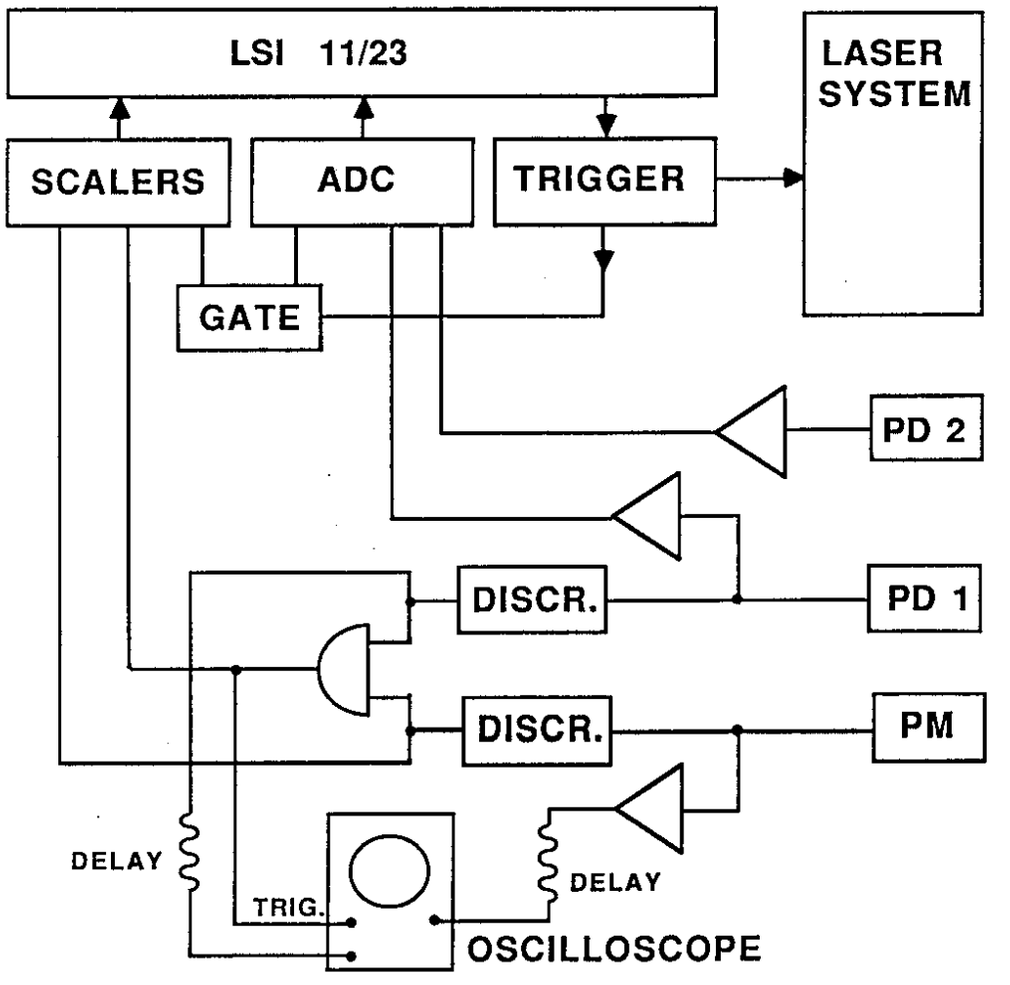
LSI 11/23
LASER SYSTEM
SCALERS
ADC
TRIGGER
GATE
PD 2
DISCR.
PD 1
DISCR.
PM
DELAY
TRIG.
DELAY
OSCILLOSCOPE

Fig. 2

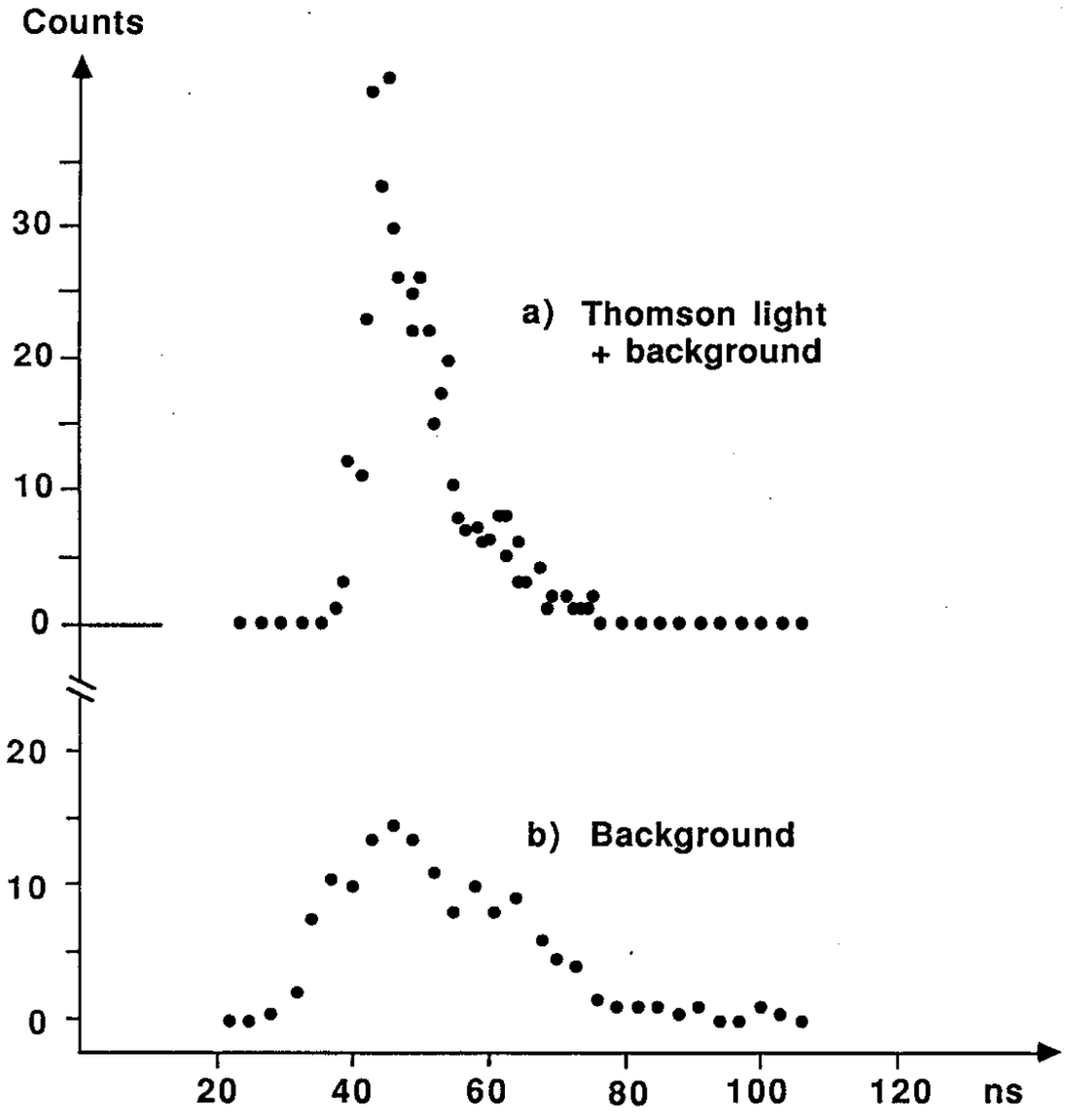
Counts
30
20
10
0
a) Thomson light
+ background
20
10
0
b) Background
20
40
60
80
100
120
ns

Fig. 3

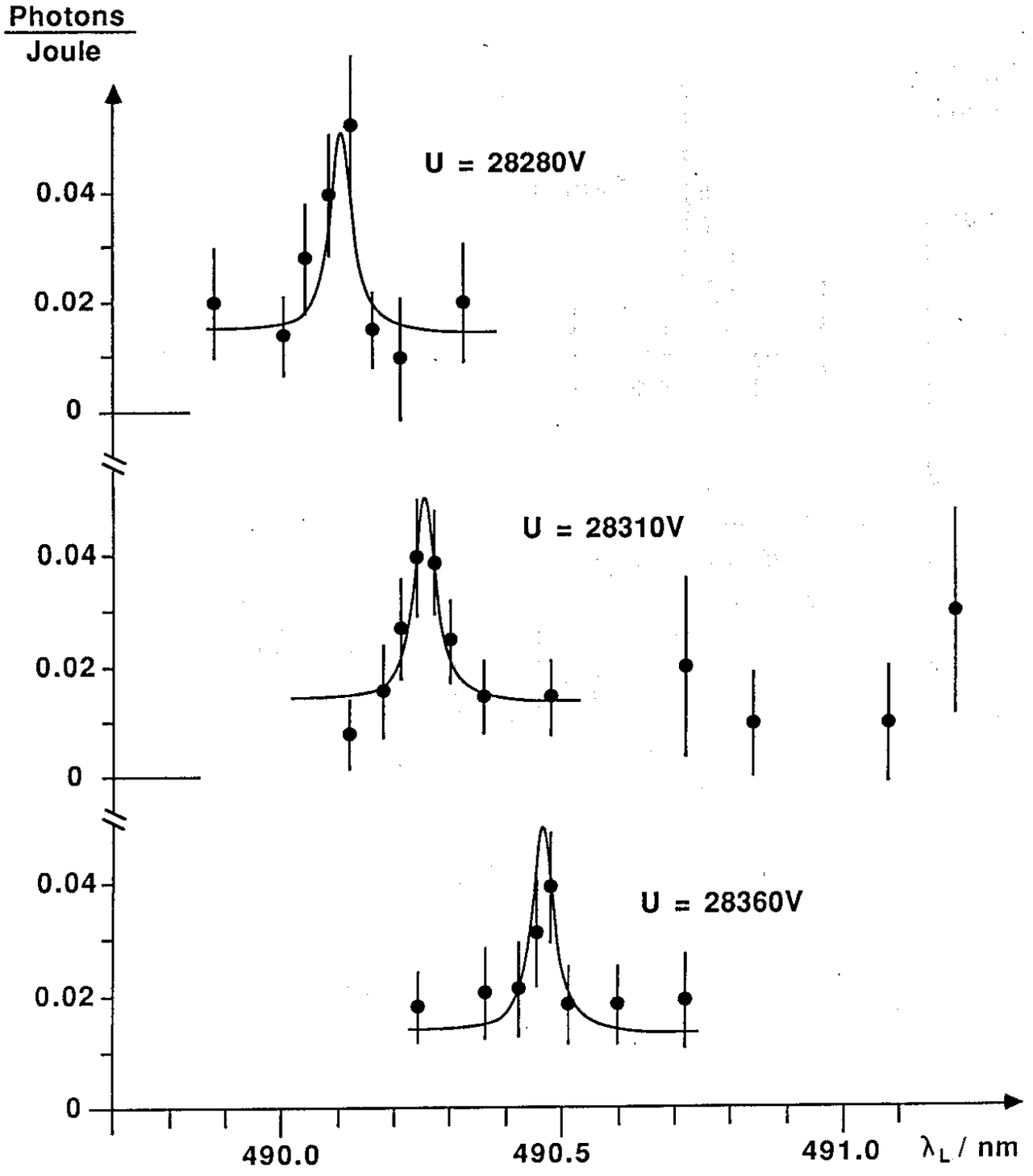
Photons
Joule
U = 28280V
U = 28310V
U = 28360V
0.04
0.02
0
0.04
0.02
0
0.04
0.02
0
490.0
490.5
491.0
λL / nm

Fig. 4

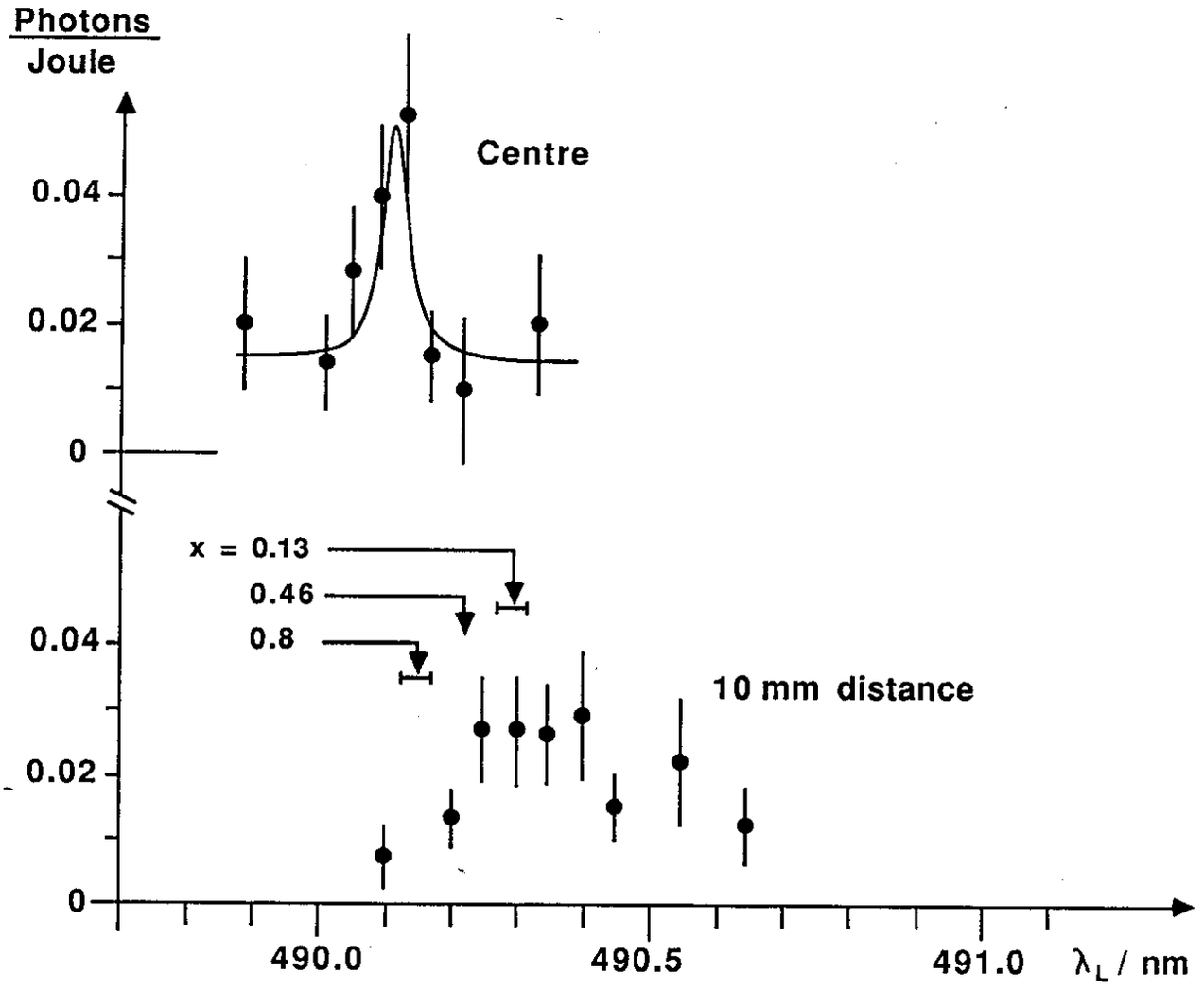
Photons
Joule
Centre
0.04
0.02
0
x = 0.13
0.46
0.8
0.04
0.02
0
10 mm distance
490.0
490.5
491.0
λL / nm

Fig. 5